Characteristics of Nanostructure Porous Silicon Prepared by Anodization Technique

Dr.Uday M. Nayef
Department of Applied Science, University of Technology/ Baghdad
E-mail: unayef@yahoo.com
Ayoub H. Jaafar
Department of Applied Science, University of Technology/ Baghdad

Received on: 4/6/2012 & Accepted on: 6/12/2012

ABSTRACT

Porous silicon (PS) layers are prepared by anodization for different current densities. The samples are then characterized the nanocrystalline porous silicon layer by X-Ray Diffraction (XRD), Atomic Force Microscopy (AFM), Fourier Transform Infrared (FTIR), Reflectivity and Raman. PS layers were formed on a p-type Si wafer. anodized electrically with a 10 and 40 mA/cm^2 current density for fixed 20 min etching times.

We have estimated crystallites size from X-Ray diffraction about nanoscale for porous silicon and AFM confirms the nanometric size and therefore optical properties about nanocrystalline silicon yields a Raman spectrum showing a broadened peak shifted below 520 cm^{-1}.

Keywords: porous silicon, X-Ray Diffraction, morphological properties, Fourier Transform Infrared, Reflectivity, Raman.

توصيف السليكون المسامي النانوي المحضر بالتقنية الانودية

الخلاصة

حضرت طبقات السليكون المسامي بالتقنية الانودية لكثافة تيار مختلفة. درست خصائص طبقات السليكون المسامي نانوية التركيب مثل الصفات التركيبية والمورفولوجية والكيميائية و البصرية (الانعكاسية ورامان). طبقات السليكون المسامي كونت على شرائح سليكون من النوع القابل. وكانت كثافة التيار المستخدم بتقنية الانودية هو ١٠ و ٤٠ ملي امبير/سم^2 وزمن تنميش ثابت ٢٠ دقيقة.

وجد ان الحجم البلوري من خلال قياسات حيود الاشعة السينية هو الحجم النانوي للسليكون المسامي و فحوصات مجهر القوة الذري اثبت ذلك وكذلك من الصفات البصرية حول التركيب النانوي للسليكون هو طيف رامان اظهر توسع وازاحة القمة عند ٥٢٠ سم$^{-1}$.

https://doi.org/10.30684/etj.31.3B.7
2412-0758/University of Technology-Iraq, Baghdad, Iraq

INTRODUCTION

Silicon has historically been the dominant material for electronics, while work in optoelectronics has relied almost entirely on III – V compound materials such as GaAs gap and InP. The primary reason for this dichotomy of materials systems has been the tenet that light emission from silicon is impractical because of its indirect band gap structure [1].

Porous silicon (PS) is conventionally formed by electrochemical anodization etching technique where the pore morphology can be easily modified by varying the fabrication parameters through an electrical bias. Some of the drawbacks of electrochemically etched PS surface are setup cost as the anodization process requires constant current source, anodization cell and its inability to process large area PS layers [2].

The terms 'anodic etching' and 'anodization' are used to describe pore formation because the semiconductor acts as the anode in the electrochemical reaction in which silicon atoms are separated from the crystal.

For PS manufacture, there are many techniques have been developed including electrochemical anodization, spark erosion, stain etching, sol-gel and vapor etching methods. Especially, the electrochemical anodization etching is the most popular method for PS manufacture. In general, the illustrative equation of the overall process during PS electrochemical etching process can be expressed as:

$$Si + 2HF + 2h+ \rightarrow SiF_2 + 2H^+ \quad \ldots\ldots\ldots\ldots (1)$$

$$SiF_2 + 4HF \rightarrow H_2 + H_2SiF_6 \quad \ldots\ldots\ldots\ldots (2)$$

According to the chemical reaction equation, there are two major parameters to affect the etching rate of fabricated PS film; one is the hole ($h+$) concentration of used Si-wafer, and the other is the electrolyte concentration of HF-based solution [3].

PS can be considered as a silicon crystal having a network of voids in it. The nanosized voids in the Si bulk result in a sponge-like structure of pores and channels surrounded with a skeleton of crystalline Si nanowires [4].

After the discovery by Canham that porous silicon can be electroluminescent at room temperature in the visible range, there has been a growing interest to study its optical properties. Porous silicon is prepared by electrochemical etching, and layers with very good quality are obtained with an adequate control of the growing parameters [5].

The meso-poreux porous silicon layer (PS) has become an interesting material owing to its potential applications in many fields including optoelectronics and photovoltaics [6].

EXPERIMENTAL DETAILS

The substrate used in this experiment is p-type (111) Si wafer with resistivity (1.5-4) Ω.cm thickness 508±15 μm grown by Czochralski (CZ). The back faces of wafers were doped with boron followed by Al metalization to improve the uniformity of current flow during anodization and to obtain homogeneous porous layers [7]. The PS sample was prepared by electrochemical anodization method in a solution of 40% hydrofluoric acid and 99.9% ethanol (V_{HF} : $V_{C_2H_4OH}$ = 1:1) at a constant current density, and the etching time was 20 min. after anodization, the sample was rinsed in ethanol and pentane and dried in argon (Ar). Ethanol is often added to the HF solution to reduce its surface tension, thereby allowing the H_2 gas formed during the reaction to escape, preventing it from sticking to the etching surface and improving the homogeneity of the resulting porous layer. Typical anodization arrangements are schematically shown in Figure (1).

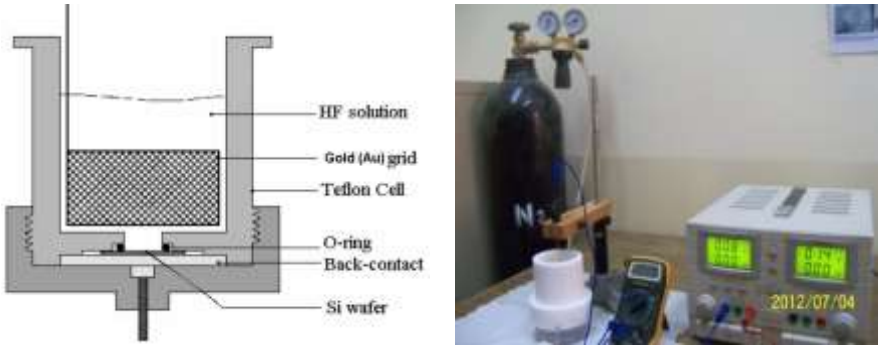

Figure (1) Schematic diagram of the porous silicon anodization.

The structure of silicon crystalline before and after anodization, as shown by XRD-6000 SHIMADZU Japan, FTIR IRAffinity-1 Fourier Transform Infrared Spectrophotometer SHIMADZU and AFM the atomic force micrographs were taken for porous silicon by AA3000 Scanning Probe Microscope Angstrom Advanced Inc.

RESULTS AND DISCUSSION

a. Structural Properties

XRD studies showed distinct variations between the bulk silicon surface and the porous silicon surfaces formed at different anodizing current densities.

The X-ray beam is diffracted at specific angular positions with respect to the incident beam depending on the phases of the sample. When crystal size is reduced toward nanometric scale, then a broadening of diffraction peaks is observed and the width of the peak is directly correlated to the size of the nanocrystalline domains [8-9]

Figure(2), shows a typical diffraction pattern of PS sample fabricated at etching current density of 10 and 40 mA/cm^2 respectively at etching time 20 min.

XRD spectra of bulk silicon showed a very sharp peak at 2θ = 28.857° showing the single crystalline nature of the wafer. This peak becomes very broad with varying full-width at half maximum (FWHM) for different anodization current densities as shown in Figure (2), which confirms the formation of pores on the crystalline silicon surface.

When the current density is increased from 10 mA/cm^2 to 40 mA/cm^2 the number of pores increased with thicker silicon walls as evident from the sharp nature of the (111) peak. Further, the presence of this peak in all the PS structures confirms that the cubic structure of the crystalline silicon is retained even after the pore formation.

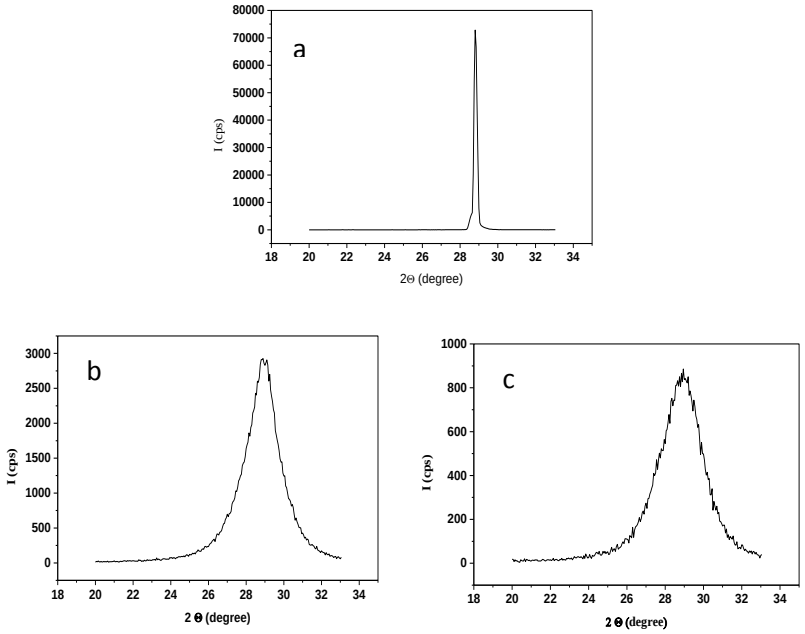

Figure (2) X-ray diffraction of porous silicon prepared by different current density at etching time 20 min (a) Si bulk (b) PS 10 mA/cm^2 (c) PS 40 mA/cm^2.

b. Morphological Properties

The surface morphology of the oxidized PS layers was investigated using Atomic force microscope (AFM) studies focus entirely on the nanoscale characterization of PS films. We have studied the surface morphology of the PS layers prepared by anodized etching observations from the AFM graphs could be distinguished. A sponge-like structure is produced.

When current density increases, a part of pores coagulate to larger structures. Figure (3) shows the 3D AFM image and diameter values distribution of PS samples prepared under different current density of porous silicon in which the irregular and

randomly distributed nanocrystalline silicon pillars and voids over the entire surface can be seen.

Table (1) shows the observed roughness, root mean square (RMS) and average diameter of pores for samples prepared under different current density.

Table (1) The calculated morphology characteristics of PS samples.

Current density (mA/cm^2)	Etching Time (min)	Roughness Ave. (nm)	RMS (nm)	Avg. Diameter (nm)
10	**20**	**0.283**	**0.342**	**17.53**
40		**1.76**	**2.13**	**24.88**

PORE MORPHOLOGY

When current flows in the electrochemical cell, the dissociation reaction localizes on a particular side of a silicon surface, thus initiating the etching of an array of pores in the silicon wafer. The pore morphology was analyzed under conditions of varying current densities. At low current density, a highly branched, randomly directed and highly interconnected meshwork of pores was obtained. However, increasing in current density orders the small pores to exhibit cylindrical shapes giving rise to larger pore diameter (Buda and Kohanoff, 1994; Beattie *et al*., 1995; Canham, 1997; Collins *et al*., 2002) [10].

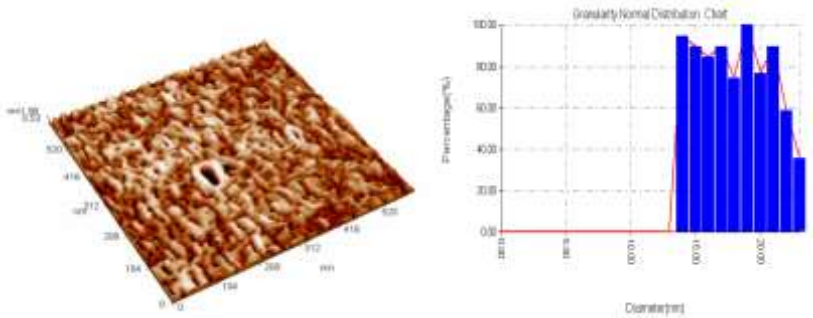

(a) 10 mA/cm^2, Avg. Diameter: 17.53 nm

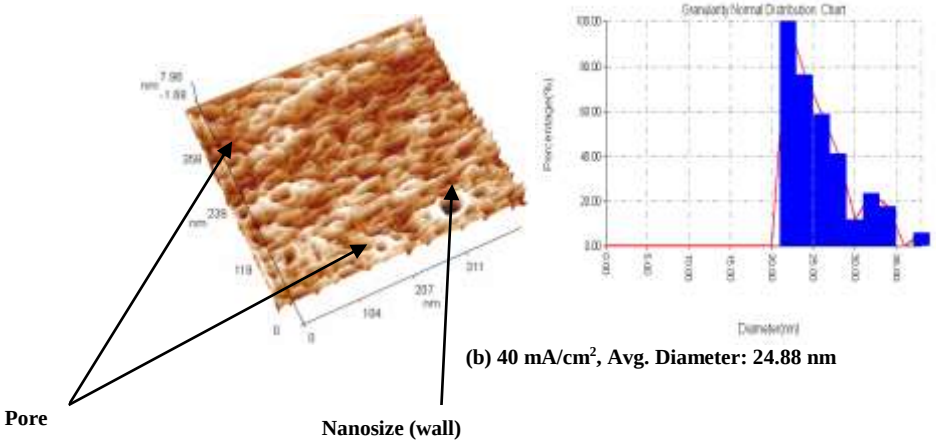

(b) 40 mA/cm^2, Avg. Diameter: 24.88 nm

Figure (3) Typical AFM image for meso-porous silicon sponge like (a) 10 and (b) 40 mA/cm^{2}at etching time 20 min.

c. Chemical Composition of PS Layer

Surface chemical composition of PS is best probed with Fourier Transform Infrared (FTIR) spectroscopy. FTIR signal in PS is larger and easier to measure than in bulk Si due to much larger specific area.

The pore surface includes a high density of dangling bonds of Si for original impurities such as hydrogen and fluorine, which are residuals from the electrolyte. Additionally, if the manufactured PS layer is stored in ambient air for a few hours, the surface oxidizes spontaneously.

Figure (4) shows, the FTIR spectra measured from samples at: (a) current density 10 mA/cm^2 and (b) current density 40 mA/cm^2 and etching time 20 min.

Chemical bonds and their IR resonance positions detected in PS are shown in Table (3).

The transmittance peak at615.29cm^{-1} Si-Si stretching in 867.97cm^{-1} Si-H_2 wagging mode, 908.47 cm^{-1} Si-H_2 scissor mode [11-12]. The peak at around 1035.7cm^{-1} is from Si-O-Si stretching modes [13], which are dependent on the oxidation degree of porous silicon. The transmittance peak at 2987.74 cm^{-1} C-H stretch (CH_3) [14-15].

Table (3) Wavenumber positions and attributions of the transmittance peaks observed in several PS samples by Fourier transform infrared absorption FTIR measurements.

Peak position (cm^{-1})	Attribution
615.29	Si-Si stretching
867.97	Si-H_2 wagging
908.47	Si-H_2 scissor
1035.77, 1112.93	Si-O stretching in O-Si-O
2088.99	Si-H stretch. (Si_3-SiH)
2113.98	Si-H stretching. (Si_2H-SiH)
2987.74	C-H stretch. (CH_3)

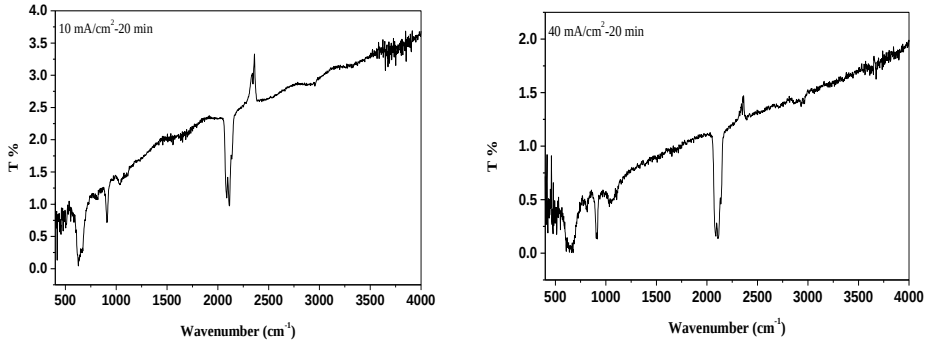

Figure (4) IR transmittance spectrum of a PS layer

(a) 10 mA/cm^2 (b) 40 mA/cm^{2}at etching time 20 min.

The porous silicon surface shows lower reflectance which is due to the very thin layer of porous silicon and changed refractive index profile at the interface of the bulk silicon and porous silicon material.

It can be seen that the reflectivity of PS is reduced with increasing the current density from (10 to 40 mA/cm^2). Hence, when current density is increased, the porosity of porous silicon layer increased, and refractive index will reduced. Thus the reflectivity of porous silicon is reduced.

Reduced reflectivity is also attributed to the light scattering and increased light trapping at wavelength (400-800 nm). The scattering light may be due to the surface roughness at the PS-Si interface, where as the roughness increased with increasing the current density. The high degree of roughness of the PS surface implies the possibility of using the porous layer as an antireflection coating for solar cells because the surface reduces the light reflection [16]. Our results are in good agreement with those of other investigators [17, 18].

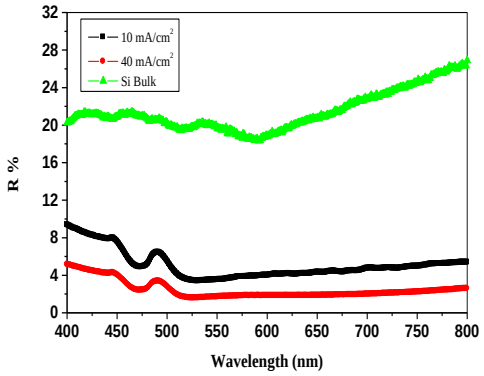

Figure(5) Reflectivity of bulk Si and PS with different current densities, 10 & 40 mA/cm^{2}at etching time 20 min.

Raman spectroscopy is a powerful tool that can be used to determine the solid state structure. The Raman spectrum for crystalline silicon consists of one sharp peak situated at 520cm^{-1}. On the other hand, Raman spectrum from amorphous silicon consists of a broad peak at 480 cm^{-1}. Nanocrystalline silicon yields a Raman spectrum showing a broadened peak shifted below 520 cm^{-1} [19].

The Raman spectra changes in porous silicon caused by chemical etching. This study shows how the structure of porous silicon changes as a result of the chemical etching.

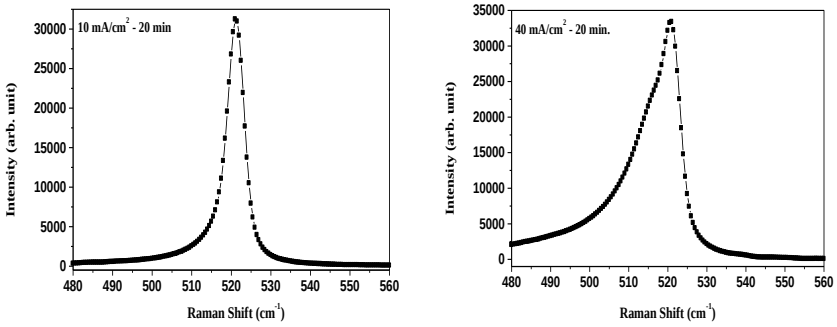

Figure (6) Raman spectra from porous silicon obtained at 10 & 40 mA/cm^2 at etching time 20 min.

CONCLUSIONS

In preparing porous silicon layers in preparing by electrochemical etching for different current densities. It can be concluded that:

1. The XRD properties showed the porous structure and the decrease of the Si nano-sized because a broadening of the Si peaks.
2. The atomic force microscopy investigation shows the rough silicon surface with increasing in current density orders the small pores to exhibit sponge like giving rise to larger pore diameter.
3. In porous silicon, as-prepared samples, oxygen is normally absent, the dominant bonds being Si-H groups (x = 1, 2 or 3).

   Which results are best and for what applications
4. porous silicon layers reduce the reflection of solar radiation in the range from (400-800) nm
5. The broadening and downshift of Raman peak towards lower energy indicates the presence of nanoscale features of the crystalline structures.

REFERENCES

[1]. Jeyakumaran, N. B. Natarajan, S. Ramamurthy and V. Vasu, "Structural and optical properties of n- type porous silicon– effect of etching time", IJNN,Vol.3, No.1, December (2007).

[2]. Biswas, J. "Growth and Characterization of Vapor Phase Stain Etched Porous Silicon"

[3]. Jia-Chuan Lin, Meng-Kai Hsu, Hsi-Ting Hou and Sin-Hong Liu, "Improvement of Photoluminescence Uniformity of Porous Silicon by using Stirring Anodization Process", World Academy of Science, Engineering and Technology 61 (2012).

[4]. Šalucha, D. K. A. J. Marcinkevičius, "Investigation of Porous Silicon Layers as Passivation Coatings for High Voltage Silicon Devices", Electronics and Electrical Engineering, No. 7(79)41-44 (2007).

[5]. Estevez, J. O. J. Arriaga, A. Me´ndez-Blas, M. G. Robles-Cha´ irez and D. A. Contreras-Solorio, "Experimental realization of the porous silicon optical multilayers based on the 1-s sequence", J. of Appl. Phys. 111, 013103 (2012)

[6]. Remache, L. A. Mahdjoub, E. Fourmond1, J. Dupuis1, M. Lemiti, "Design of porous silicon /PECVD SiOx antireflection coatings for silicon solar cells", *International Conference on* Renewable Energies and Power Quality (ICREPQ'10) Granada (Spain), 23th to 25th March, (2010).

[7]. Salcedo,W. J. F. J. R. Fernandez, E. Galeazzo, "Structural Characterization of Photoluminescent Porous Silicon with FTIR Spectroscopy", Brazilian Journal of Physics, Vol. 27, No. 4, 158-161(1997).

[8]. Lorusso,A. V. Nassisi, G. Congedo, N. Lovergine, L. Velardi, P. Prete, "Pulsed plasma ion source to create Si nanocrystals in SiO_2 substrates", Applied Surface Science, 255, 5401-5404 (2009).

[9]. Russo,L. F. Colangelo, R. Cioffi, I. Rea and L. De Stefano, "A Mechanochemical Approach to Porous Silicon Nanoparticles Fabrication", Materials 4, 1023-1033 (2011).

[10]. Patel,A. K. "Use of Electrochemically Machined Porous Silicon to Trap Protein Molecule", J. of Appl. Sci., Engineering and Technology 2(3): 208-215, (2010).

[11]. Bisi,O. S. Ossicini and L. Pavesi, "porous silicon: a quantum sponge structure for silicon based optoelectronics", Surface science reports 264, (2000).

[12]. Arce, R. D. R.R. Koropecki, G. Olmos, A.M. Gennaro, J.A. Schmidt, "Photoinduced Phenomena in Nanostructured Porous Silicon", Thin Solid Films 510, 169-174 (2006).

[13]. Zhao, Y. D. Yang, D. Li, M. Jiang, "Annealing and amorphous silicon passivation of porous silicon with blue light emission", Applied Surface Science 252, 1065–1069 (2005).

[14]. PAP, A. E. "Investigation of Pristine and Oxidized Porous Silicon", Thesis University of Oulu, (2005).

[15]. Dimova, D. - Malinovska, "Application of Stain Etched Porous Silicon in c-Si Solar Cells", Optoelectronics Review 8(4), 353-355 (2000).

[16]. Ramizy,A. Z. Hassan, K. Omar, Y. Al-Dourib , M.A. Mahdi, "New Optical Features to Enhance Solar Cell Performance Based on Porous Silicon Surfaces", Applied Surface Science 257,6112–6117, (2011).

[17]. Dubey, R. S. D. K. Gautam, "Synthesis and Characterization of Nanocrystalline Porous Silicon Layer for Solar Cells Applications", Optoelectronic and Biomedical Materials Vol. 1, Issue 1, 8-14, (2009).

[18]. Salman, K. A. Z. Hassan, K. Omar, "Effect of Silicon Porosity on Solar Cell Efficiency", Int. J. Electrochem. Sci.,7, 376 – 386, (2012).

[19]. Ohmukai, M. N. Uehara, T. Ymasaki, Y. Tsutsumi, "The effects of chemical etching of porous silicon on Raman spectra", Czechoslovak Journal of Physics, Vol. 54, No.7,781-784, (2004).